Electronic Supplementary Information

On the Validity of Rapid Optical Sensing of Dioxygen by Means of Sensitivity, Stability, and Reversibility for Archetype MOFs Post-synthetically Modified with Eu^{3+}

Thomas Kasper, Matilde Pavan, Klaus Müller-Buschbaum

Table of contents

Images of Crystal Structures 2
X-Ray Powder Diffraction of synthesized MOFs 5
Photoluminescence emission spectra 9
Stern-Volmer plot data 10
Kinetic plots according to “two site model” 11
Additional sensor cycling measurements 14
X-Ray Powder Diffraction of MOFs after oxygen sensing experiments 16
Microwave plasma atomic emission spectroscopy 17
References 17

Images of Crystal Structures

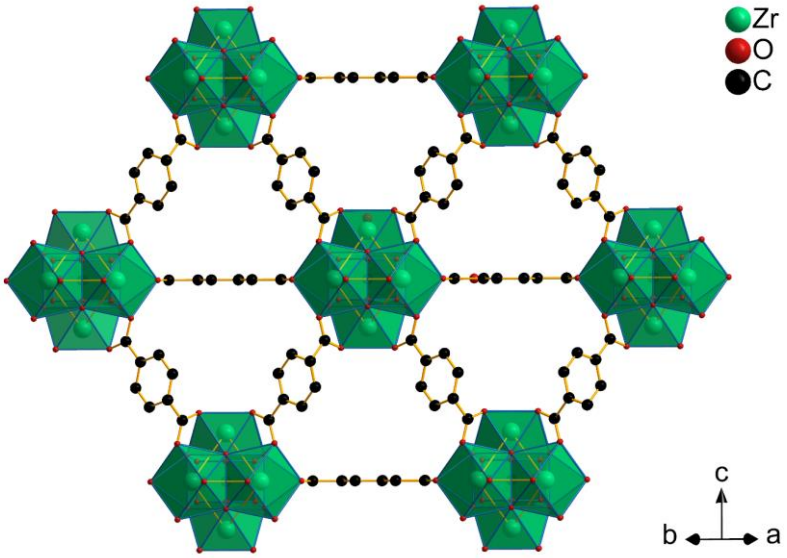

Figure S1: *Crystal structure of UiO-66(Zr). Hydrogen omitted for clarity. Image based on structure according to Ref.[1].*

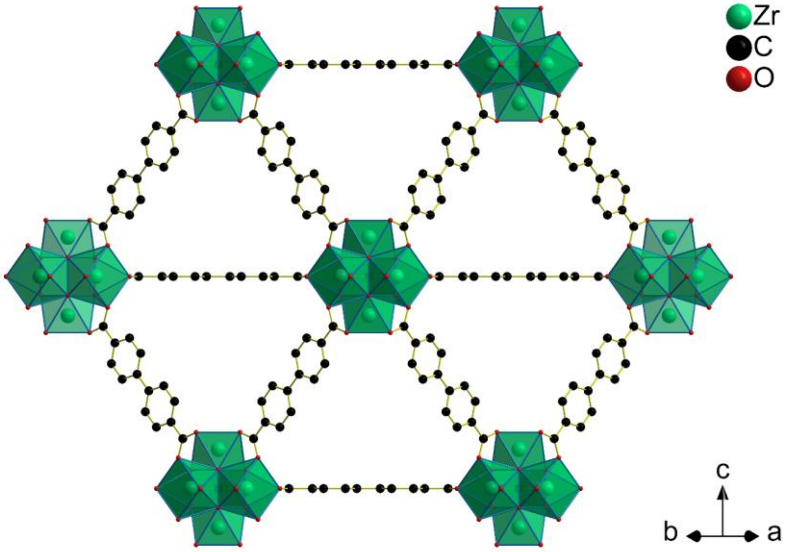

Figure S2: *Crystal structure of UiO-67(Zr). Hydrogen atoms omitted for clarity. Image based on structure according to Ref.[1]*

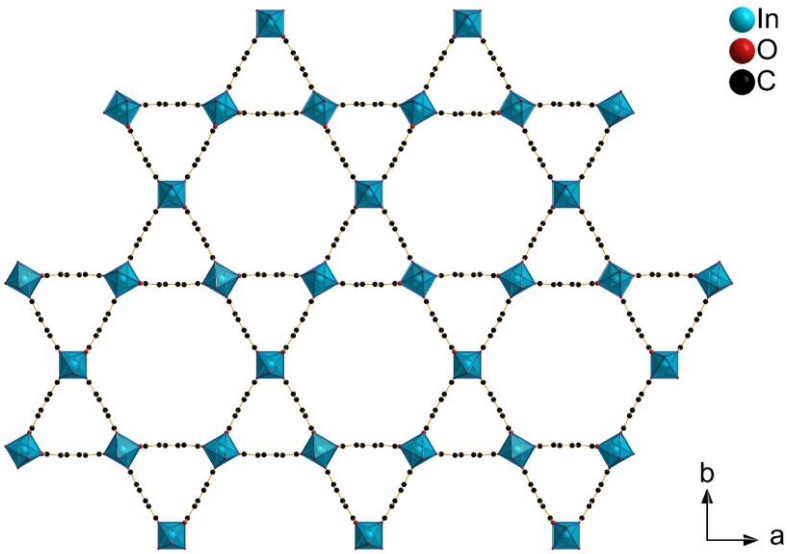

Figure S3: *Crystal structure of MIL-68(In). Hydrogen atoms omitted for clarity. Image based on structure according to Ref.* [2]

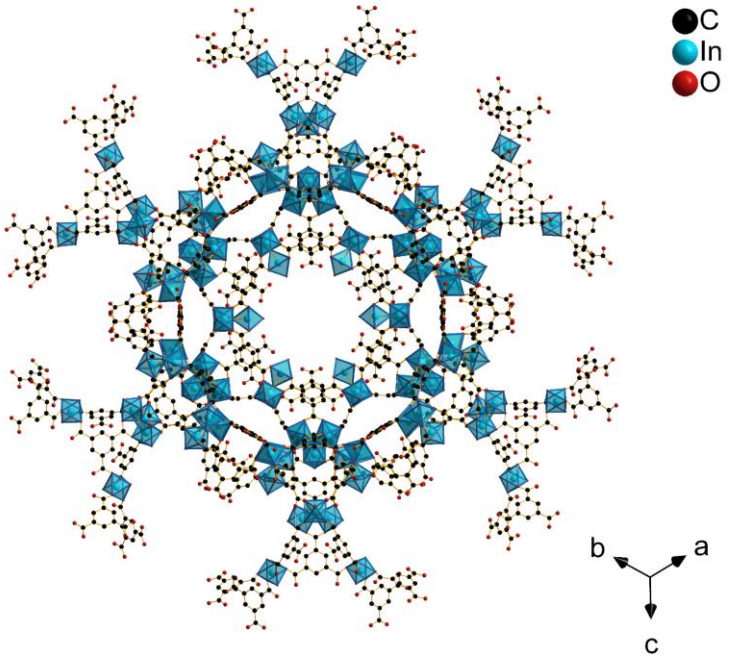

Figure S4: *Crystal structure of MIL-100(In). Hydrogen atoms omitted for clarity. Image based on structure according to Ref.*[3]

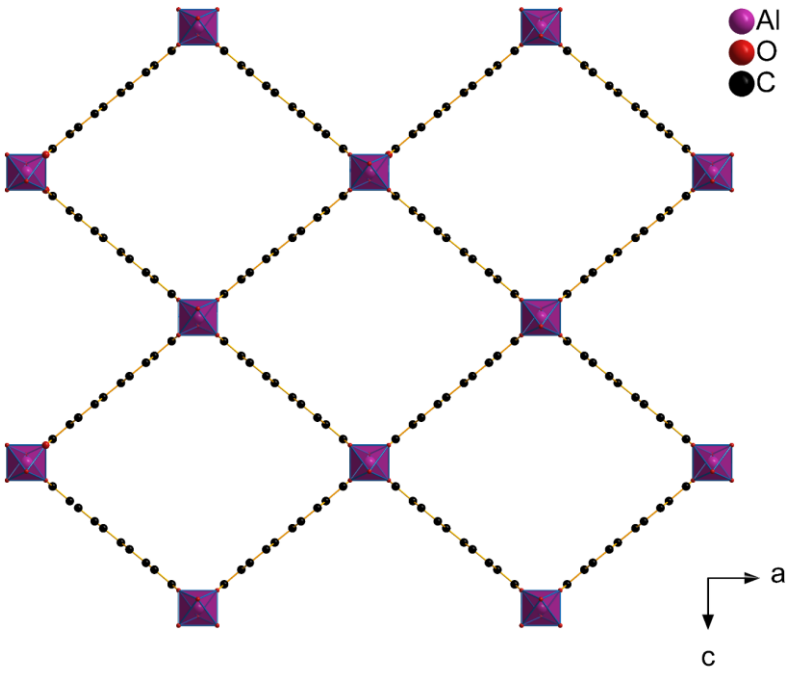

Figure S5: *Crystal structure of DUT-5(Al). Hydrogen atoms omitted for clarity. Image based on structure according to Ref.[4]*

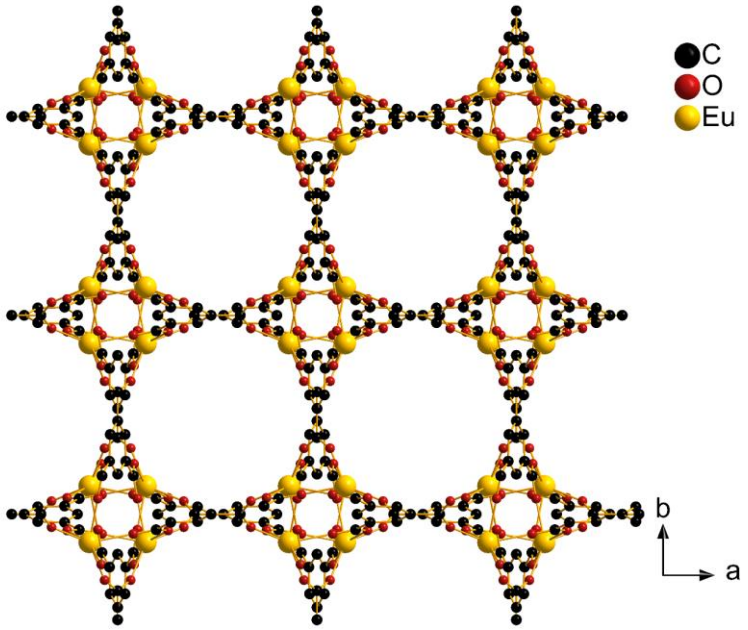

Figure S6: *Crystal structure of MOF-76(Eu). Hydrogen atoms omitted for clarity. Image based on structure according to Ref.[5]*

X-Ray Powder Diffraction of synthesized MOFs

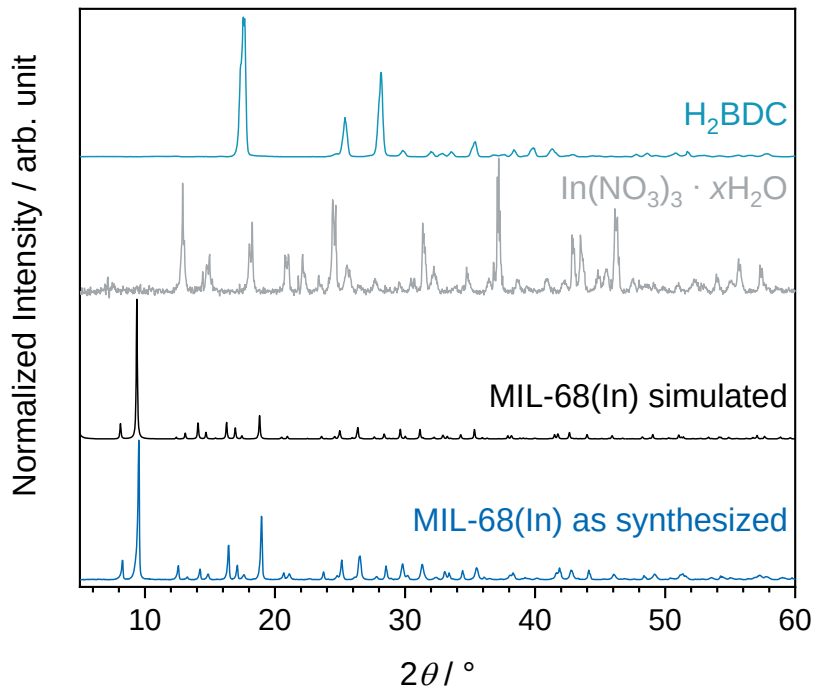

Figure S7. *X-ray powder diffractograms of as-synthesized MIL-68(In) compared to simulated and recorded and diffractograms of reagents.*[2]

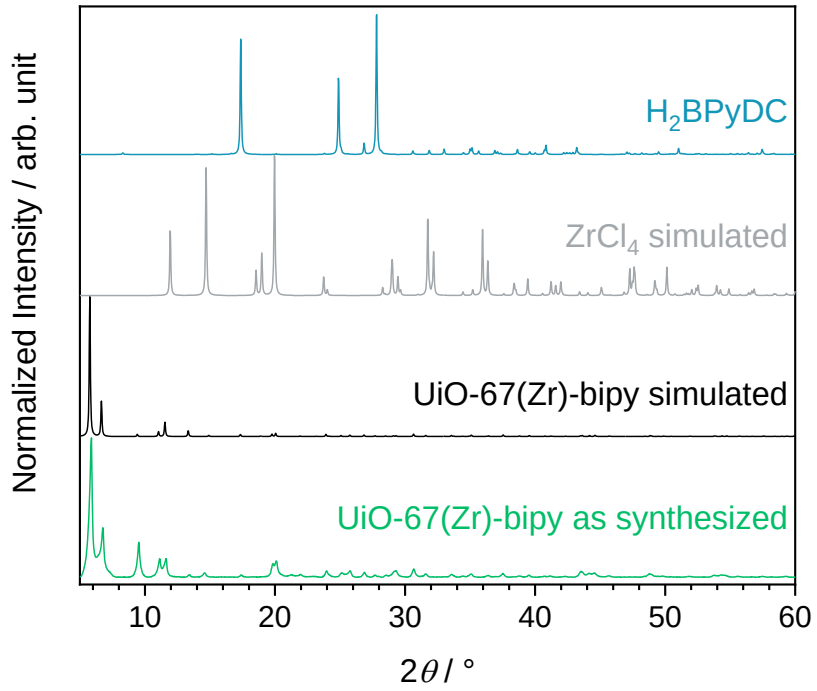

Figure S8. *X-ray powder diffractograms of as-synthesized UiO-67(Zr)-bipy compared to simulated and recorded and diffractograms of reagents.*[1,6]

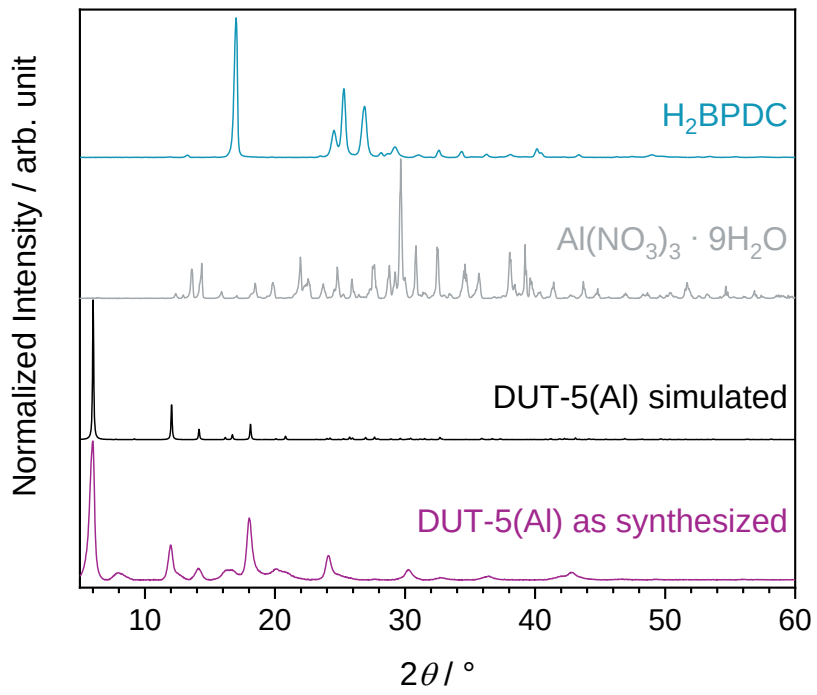

Figure S9. *X-ray powder diffractograms of as-synthesized DUT-5(Al) compared to simulated and recorded and diffractograms of reagents.*[4]

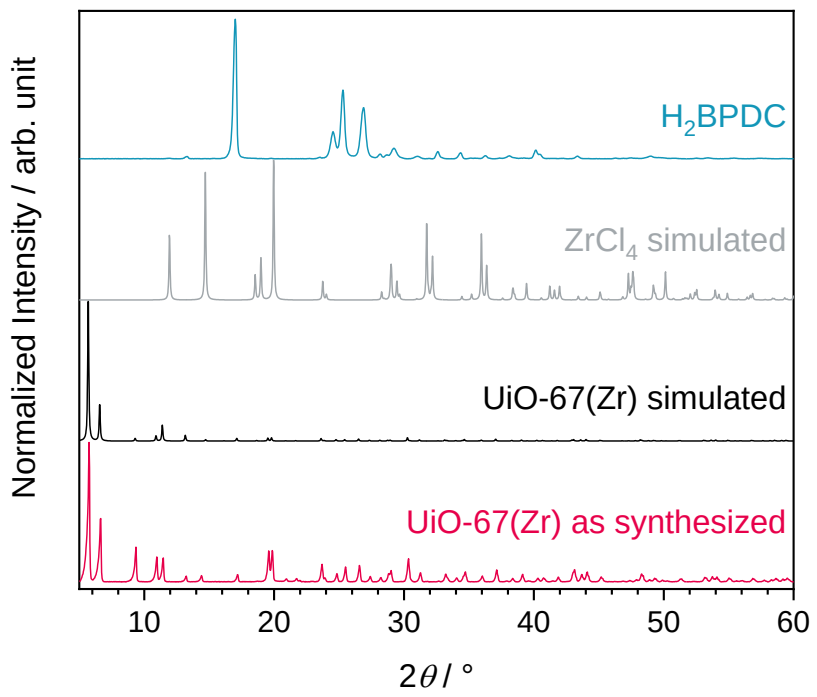

Figure S10. *X-ray powder diffractograms of as-synthesized UiO-67(Zr) compared to simulated and recorded and diffractograms of reagents.*[1,6]

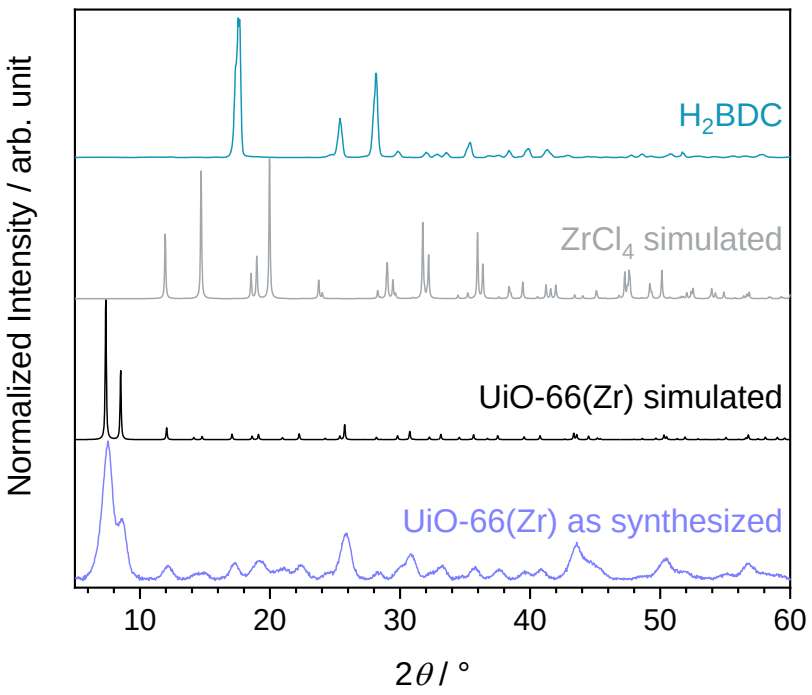

Figure S11. *X-ray powder diffractograms of as-synthesized UiO-66(Zr) compared to simulated and recorded and diffractograms of reagents.*[1,6]

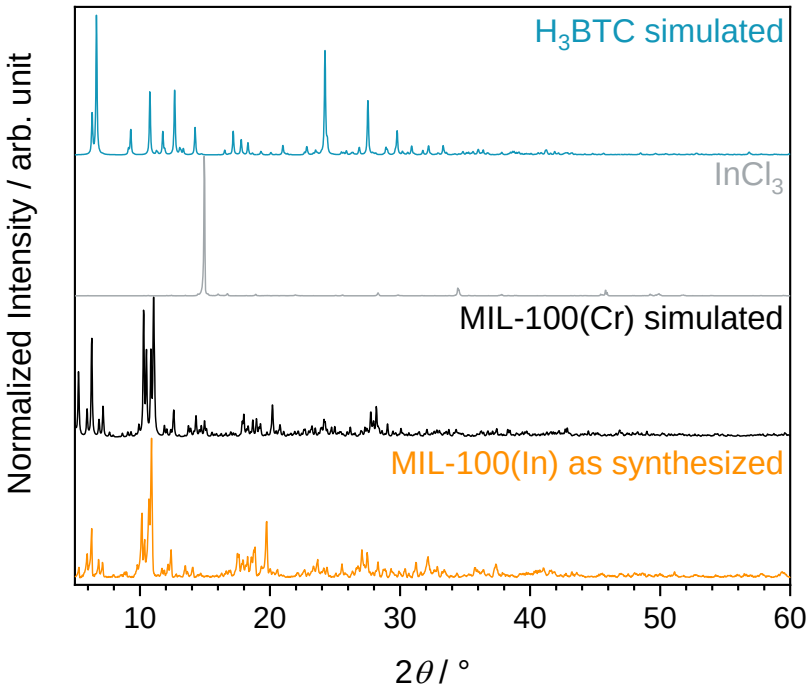

Figure S12. *X-ray powder diffractograms of as-synthesized MIL-100(In) compared to simulated and recorded and diffractograms of reagents.*[3,7]

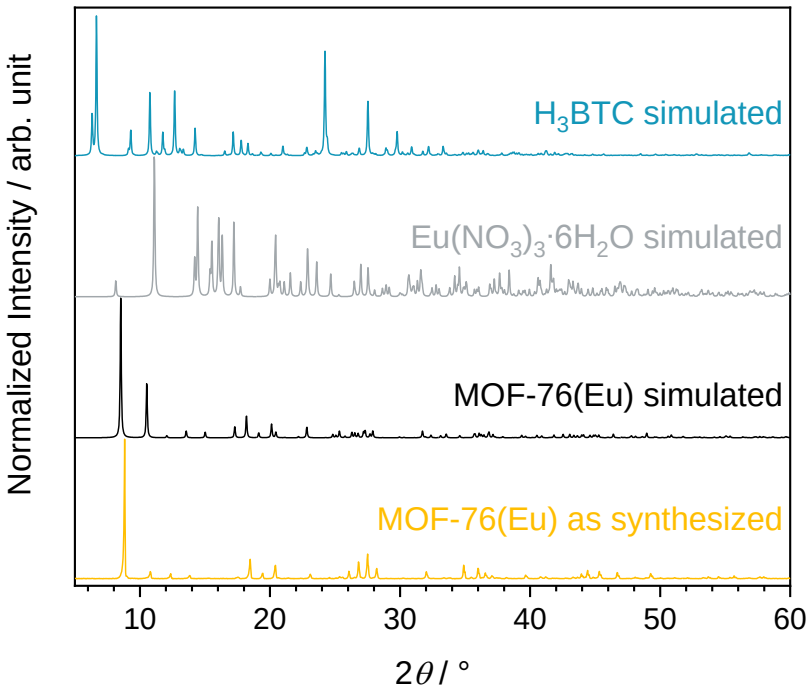

Figure S13. *X-ray powder diffractograms of as-synthesized MOF-76(Eu) compared to simulated and recorded and diffractograms of reagents.*[5,7]

Photoluminescence emission spectra

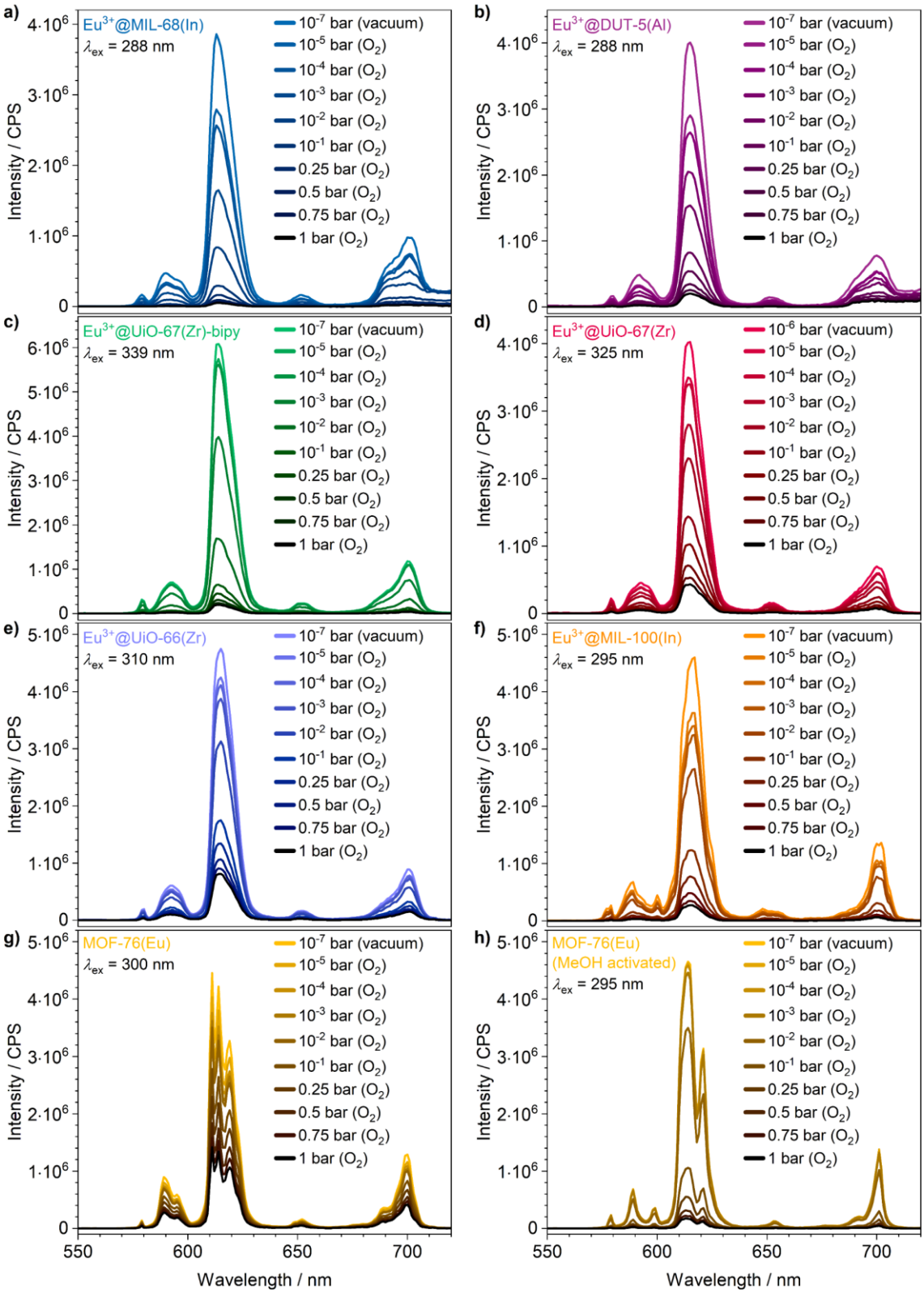

Figure S14: *Luminescence emission quenching by intensity decrease of a-f) the impregnated MOFs and g) as synthesized and h) methanol-exchanged MOF-76(Eu) under different oxygen pressures.*

Stern-Volmer plot data

Table S1. *Fitted equation of Stern-Volmer plots, plotted pressure regions and corresponding R^2 values.*

Sample	Linear equation of fit	p	R^2
Eu^{3+}@MIL-68(In)	$\frac{I_0}{I} - 1 = 10.61 \cdot p + 4.63$	0.2 bar until 1.02 bar	0.9976
Eu^{3+}@UiO-67(Zr)-bipy	$\frac{I_0}{I} - 1 = 5.32 \cdot p + 2.08$	0.1 bar until 1.02 bar	0.9991
Eu^{3+}@DUT-5(Al)	$\frac{I_0}{I} - 1 = 9.65 \cdot p + 2.09$	0.1 bar until 1.02 bar	0.9984
Eu^{3+}@UiO-67(Zr)	$\frac{I_0}{I} - 1 = 7.64 \cdot p + 0.69$	$1 \cdot 10^{-3}$ bar until 1.02 bar	0.9977
Eu^{3+}@UiO-66(Zr)	$\frac{I_0}{I} - 1 = 3.66 \cdot p + 1.33$	$5 \cdot 10^{-2}$ bar until 1.02 bar	0.9810
Eu^{3+}@MIL-100(In)	$\frac{I_0}{I} - 1 = 17.17 \cdot p + 0.63$	$1 \cdot 10^{-3}$ bar until 1.02 bar	0.9988
MOF-76(Eu)	$\frac{I_0}{I} - 1 = 1.88 \cdot p + 0.37$	$1 \cdot 10^{-2}$ bar until 1.02 bar	0.9922

Kinetic fits according to "two site model"

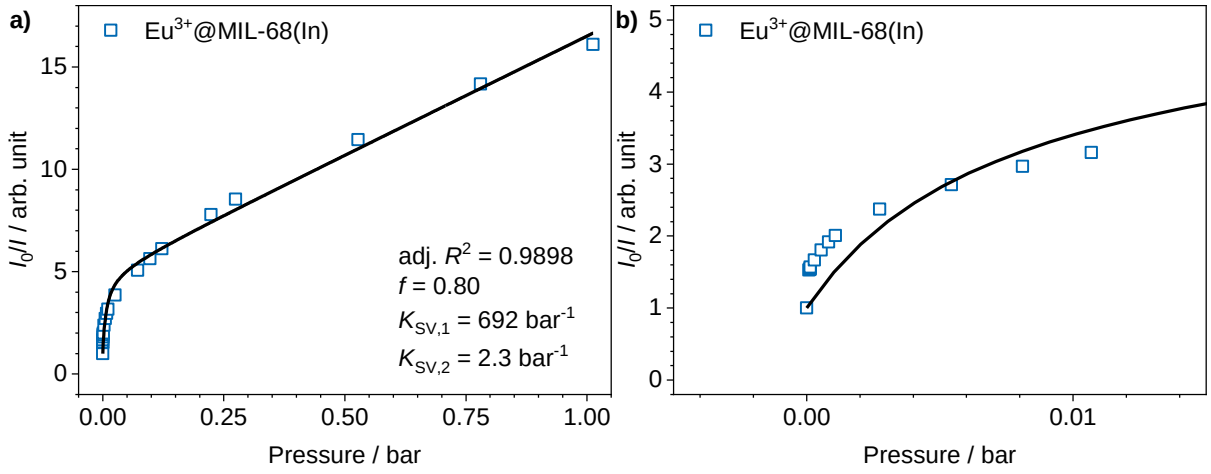

Figure S15: *a) Kinetic fit according to "two site model" and b) enlarged view of points at low pressures for Eu^{3+}@MIL-68(In).*

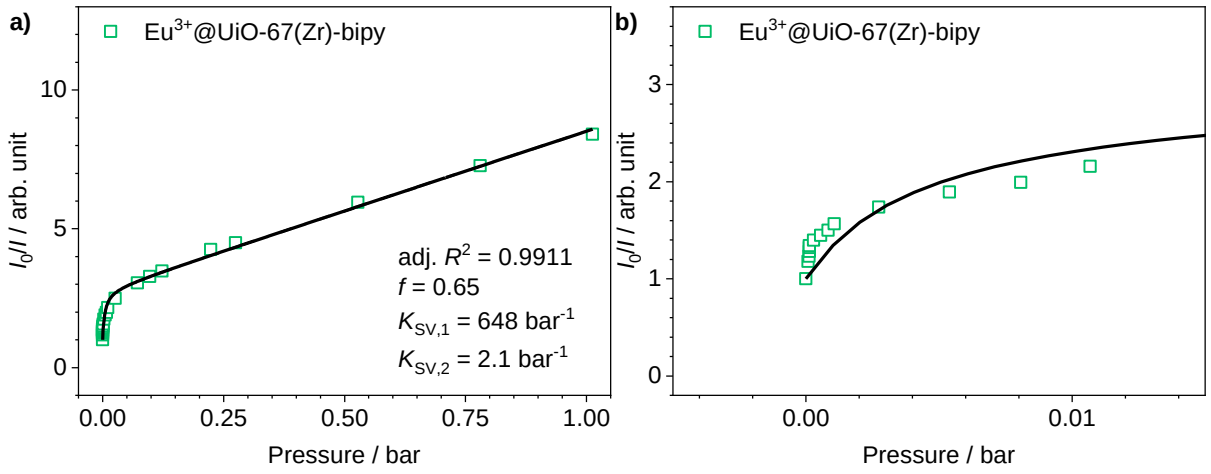

Figure S16: *a) Kinetic fit according to "two site model" and b) enlarged view of points at low pressures for Eu^{3+}@UiO-67(Zr)-bipy.*

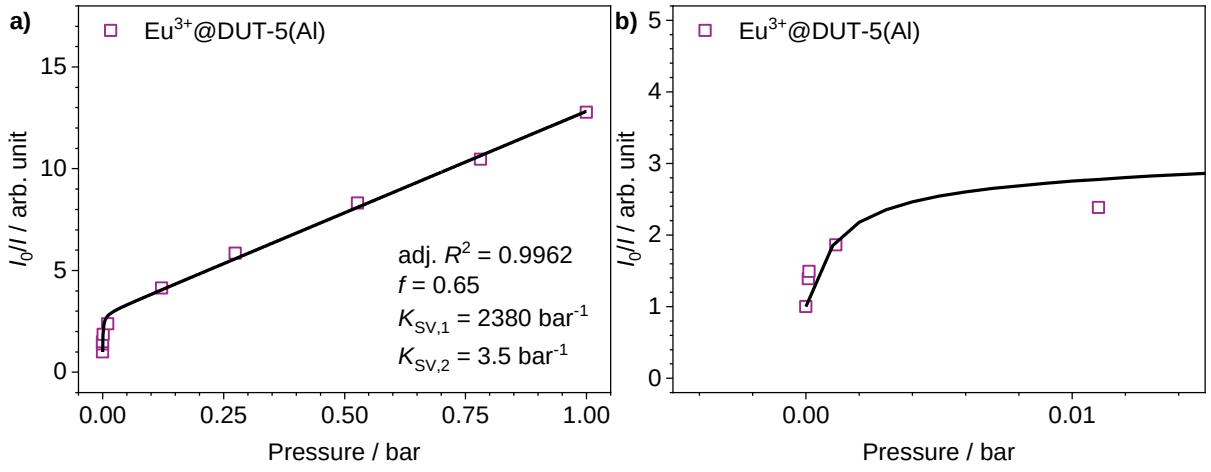

Figure S17: *a) Kinetic fit according to "two site model" and b) enlarged view of points at low pressures for Eu^{3+}@DUT-5(Al).*

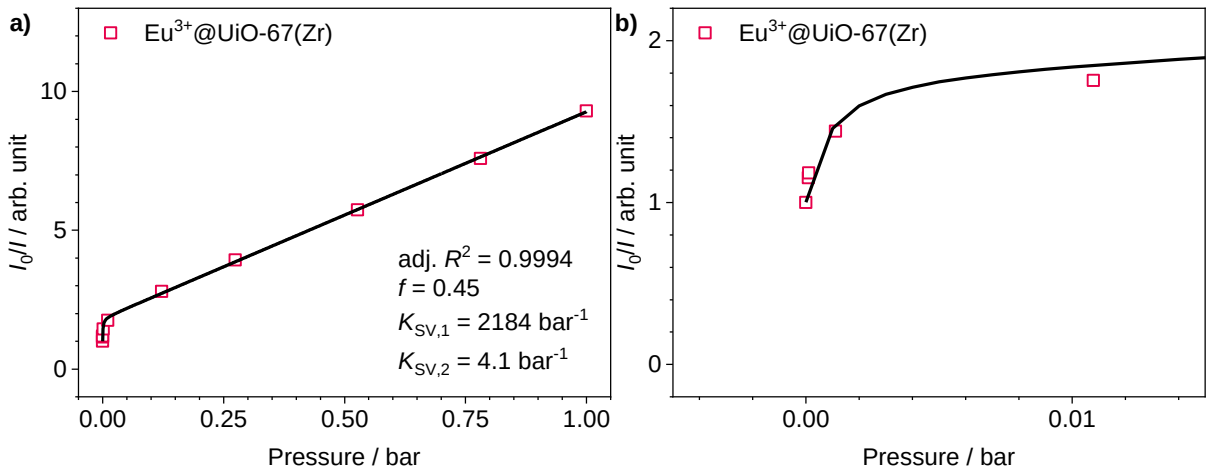

Figure S18: *a) Kinetic fit according to "two site model" and b) enlarged view of points at low pressures for Eu³⁺@UiO-67(Zr).*

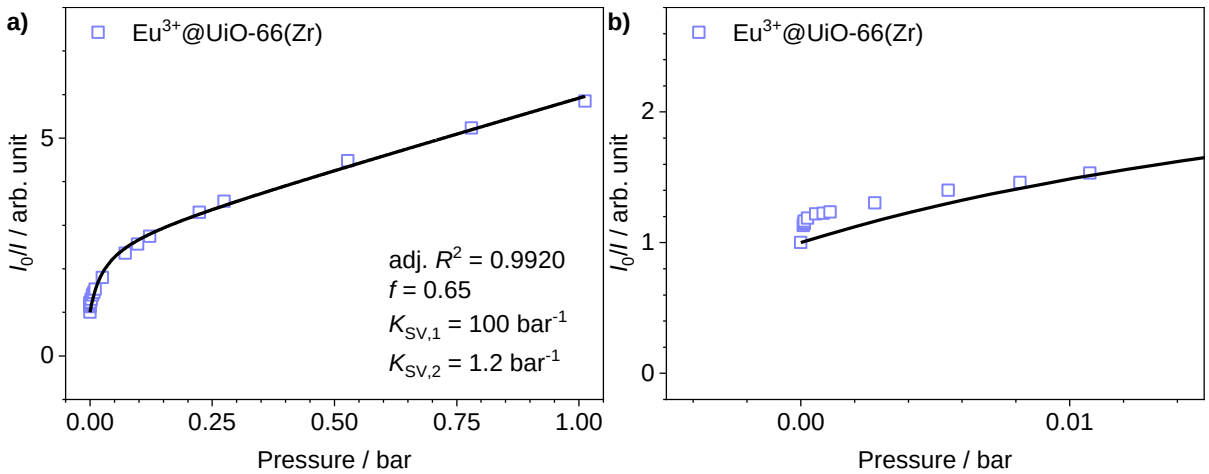

Figure S19: *a) Kinetic fit according to "two site model" and b) enlarged view of points at low pressures for Eu³⁺@UiO-66(Zr).*

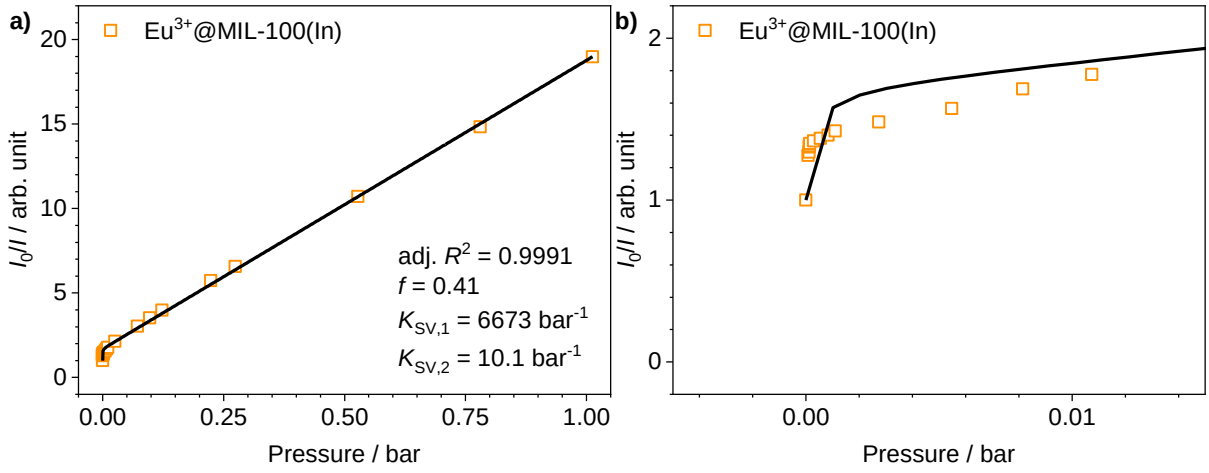

Figure S20: *a) Kinetic fit according to "two site model" and b) enlarged view of points at low pressures for Eu³⁺@MIL-100(In).*

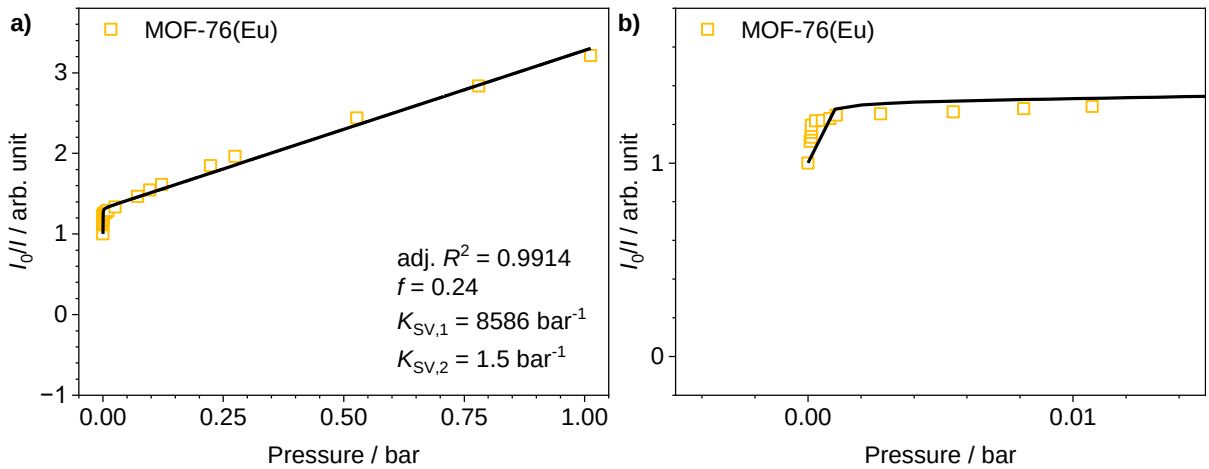

Figure S21: *a) Kinetic fit according to "two site model" and b) enlarged view of points at low pressures for MOF-76(Eu).*

Additional sensor cycling measurements

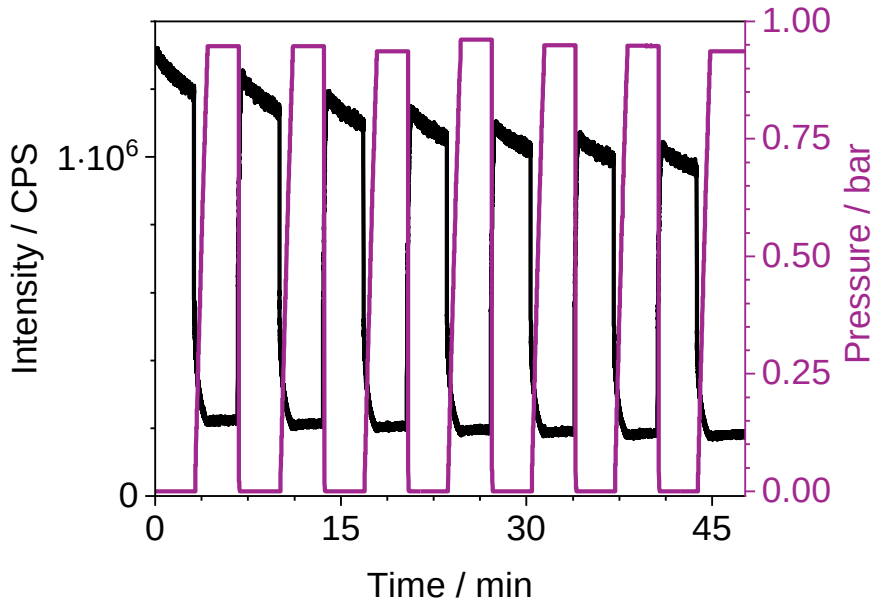

Figure S22: *Oxygen sensor cycling investigation on Eu^{3+}@DUT-5(Al).*

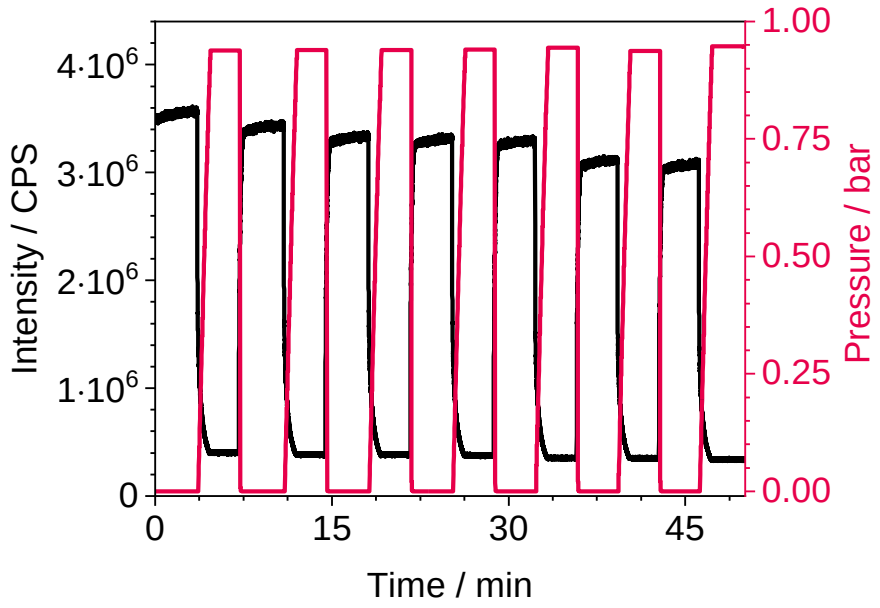

Figure S23: *Oxygen sensor cycling investigation on Eu^{3+}@UiO-67(Zr).*

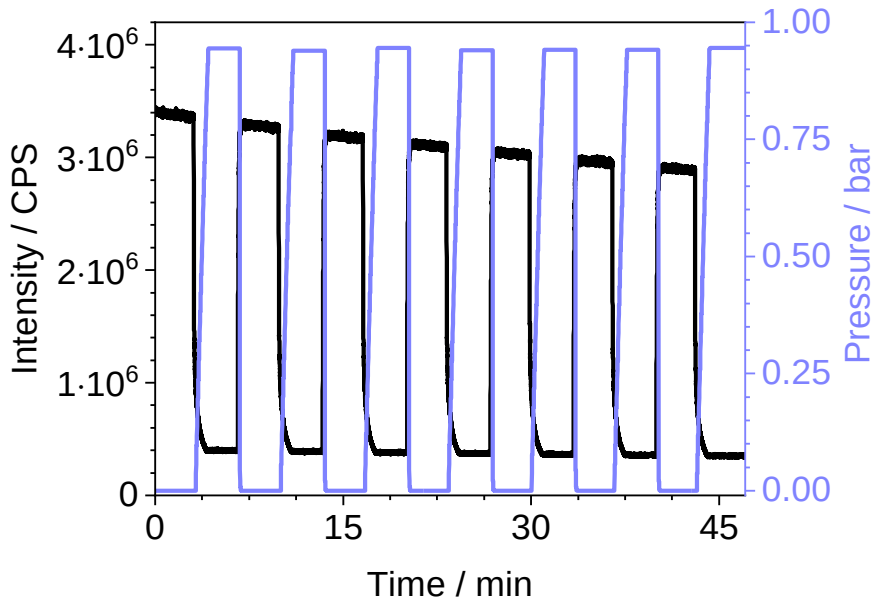

Figure S24: *Oxygen sensor cycling investigation on Eu^{3+}@UiO-66(Zr).*

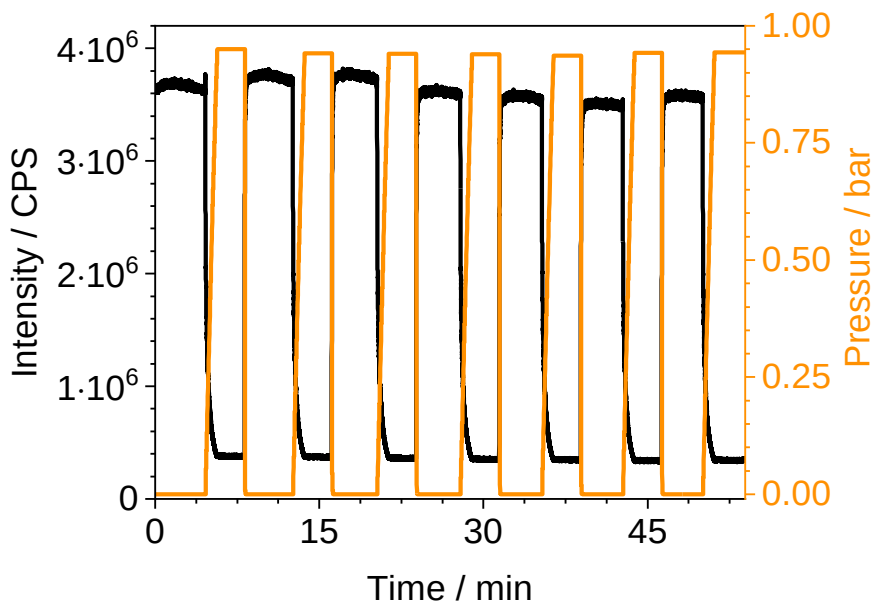

Figure S25: *Oxygen sensor cycling investigation on Eu^{3+}@MIL-100(In).*

X-Ray Powder Diffraction of MOFs after oxygen sensing experiments

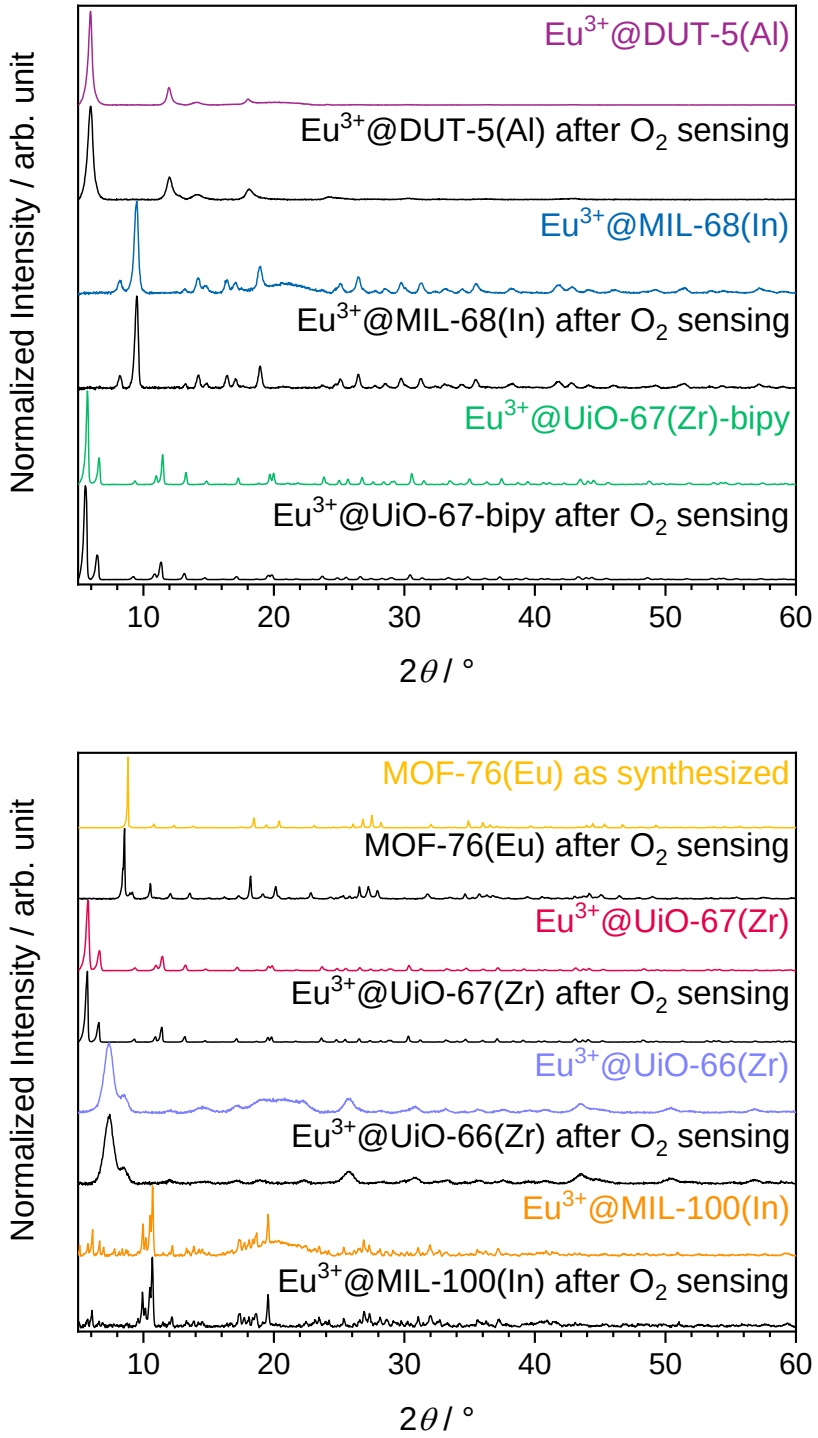

Figure S26. *Powder diffractograms of MOFs directly after impregnation and after oxygen sensing experiments.*

Microwave plasma atomic emission spectroscopy

Table S2: *Eu^{3+} content of impregnated MOFs determined with MP-AES.*

Sample	Eu^{3+} / wt%
Eu^{3+}@MIL-68(In)	<1
Eu^{3+}@UiO-67(Zr)-bipy	<1
Eu^{3+}@DUT-5(Al)	1
Eu^{3+}@UiO-67(Zr)	<1
Eu^{3+}@UiO-66(Zr)	1
Eu^{3+}@MIL-100(In)	<1

References

1 S. Øien, D. Wragg, H. Reinsch, S. Svelle, S. Bordiga, C. Lamberti and K. P. Lillerud, *Crystal Growth & Design*, 2014, **14**, 5370–5372.

2 C. Volkringer, M. Meddouri, T. Loiseau, N. Guillou, J. Marrot, G. Férey, M. Haouas, F. Taulelle, N. Audebrand and M. Latroche, *Inorg. Chem.*, 2008, **47**, 11892–11901.

3 G. Férey, C. Serre, C. Mellot-Draznieks, F. Millange, S. Surblé, J. Dutour and I. Margiolaki, *Angewandte Chemie International Edition*, 2004, **43**, 6296–6301.

4 I. Senkovska, F. Hoffmann, M. Fröba, J. Getzschmann, W. Böhlmann and S. Kaskel, *Microporous and Mesoporous Materials*, 2009, **122**, 93–98.

5 J. Yang, Q. Yue, G.-D. Li, J.-J. Cao, G.-H. Li and J.-S. Chen, *Inorg. Chem.*, 2006, **45**, 2857–2865.

6 R. Borjas Nevarez, S. M. Balasekaran, E. Kim, P. Weck and F. Poineau, *Acta Cryst C*, 2018, **74**, 307–311.

7 D. J. Duchamp and R. E. Marsh, *Acta Cryst B*, 1969, **25**, 5–19.